Modeling of compressible turbulence

By O. Zeman

1. Objectives

The work is directed toward understanding and modeling compressibility effects in turbulent flows. The primary objective is to investigate how compressibility influences the basic turbulence processes such as turbulence production and dissipation, length scale modification, spectral energy transfer, etc. The second objective is to develop parameterization schemes and models to incorporate compressibility into one-point closure models and into the subgrid scale models for LES techniques.

The ultimate purpose of this research is to develop compressible turbulence models which are capable of handling the hypersonic regime. Specifically, the emphasis will be on the model capability of predicting a) heat and momentum transfer in hypersonic boundary layers, and b) mixing and growth of high Mach number shear layers, jets and wakes.

2. Accomplishments

The work described in the following section (2.1) is an abbreviated version of the paper Zeman (1989). Section 2.2 is a part of a paper in preparation.

2.1. Dilatation dissipation: the theory and applications in modeling compressible turbulent flows

2.1.1. Abstract

The concept of dilatation dissipation ϵ_d is predicated on the existence of shock-like structures embedded within energetic turbulent eddies. On this assumption a parametric expression for ϵ_d is found $\epsilon_d = \left(q^3/L\right) F(M_t, K)$ containing calculable parameters of a turbulent field: Favre-averaged turbulence energy $q^2 = \widetilde{u_j u_j}$, length scale L, and r.m.s. (turbulent) Mach number M_t. The function $F(M_t, K)$ is a measure of the probability of ϵ_d with respect to the solenoidal dissipation (q^3/L), and involves integration over the p.d.f. of fluctuating velocity. K is the kurtosis, or intermittency factor, of the fluctuating field. The dilatation dissipation is incorporated in a second-order closure model for compressible mixing layers and the model predictions of mean and turbulence quantities are compared with experiments. The model is capable of predicting the reduction of layer growth rates as a function of the convective Mach number M_c in experiments. The Mach number effect on the turbulence structure is demonstrated by comparing the computed centerline turbulence intensities with the measurements of Samimy and Elliott (1989) and Samimy et al. (1989) for M_c between 0.51 and 0.86.

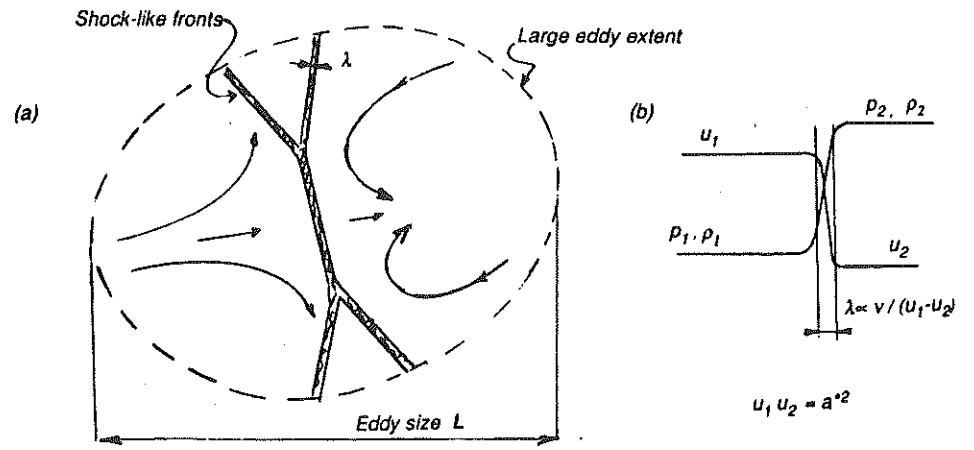

FIGURE 1. (a) Sketch of shock-like structure in a turbulent eddy; (b) normal shock relations.

2.1.2 Theoretical model for dilatation dissipation

The compressible, homogenous, turbulence field can be described in terms of solenoidal and dilatational components of velocity, i.e., $u_i = u_{si} + u_{di}$, where u_s and u_d satisfy the constraints $\nabla \cdot \mathbf{u}_s = 0$, and $\nabla \times \mathbf{u}_d = 0$. Then, in high Reynolds number approximation, the Favre-averaged second-order equations for (decaying) homogeneous turbulence can be written as (Zeman, 1989)

$$1/2 \frac{\partial q^2}{\partial t} = -\nu \overline{\omega_k \omega_k} - 4/3 \nu \overline{\theta^2} + \rho^{-1} \overline{p\theta} \tag{1}$$

$$c_p \frac{\partial T}{\partial t} = -1/2 \frac{\partial q^2}{\partial t} \tag{2}$$

$$\overline{p} = \overline{\rho} R T \tag{3}$$

The viscous term $\nu \overline{\omega_k \omega_k}$ (labeled ϵ_s for future reference) is the traditional solenoidal dissipation due to the energy cascade to small scales and depends only on u_s; the second viscous term in (1) is proportional to the square of fluctuating divergence $\theta = u_{j,j}$, and we shall call it the *dilatation dissipation* ϵ_d. In the energy equation (2), T is the Favre-averaged (mean) temperature and the sum of (1) and (2) yields the enthalpy conservation law $c_p T + \frac{1}{2} q^2 = c_p T_o = \text{const}$. By dimensional analysis, it is then expected that the decay of compressible turbulence be described by

$$\frac{\partial q^2}{\partial t} = -\frac{q^3}{L} f(M_t)$$

where f is a function of the turbulent Mach number $M_t = q/a$ based on the sonic velocity $a = \sqrt{\gamma R T}$, and L is a turbulence length scale so that the solenoidal dissipation $\epsilon_s \propto q^3/L$.

In direct numerical simulation of compressible 2D turbulence, Passot and Pouquet (1987) found that for sufficiently large initial density fluctuation levels $\rho'/\overline{\rho}$ and turbulent Mach number $M_t > 1$ the computed field of initially solenoidal turbulence evolved into a shock-like structure as sketched in Figure 1. Thin regions of steep density gradients (shock-like structures) are embedded in large scale vortices (of length scale L). The shock-like structure may be considered quasi-stationary with the instantaneous dissipation rate $\nu\theta^2 = \nu(\triangle u/\lambda)^2$ where $\triangle u$ is a normal velocity difference across the steep density interface which has a thickness λ. This thickness is determined by the Reynolds number relationship $\lambda\triangle u/\nu = O(1)$ and velocities upstream and downstream of the normal shock are related by the Prandtl-Meyer relation:

$$u_1 u_2 = a*^2 = \gamma R T^* = u_1^2(1 - \triangle u/u_1). \tag{4}$$

where $a*$ is the sonic velocity at the "sonic" temperature $T^* = 2T/(\gamma + 1)$, (with respect to the turbulence frame of reference moving with the local mean flow velocity). The volume fraction occupied by the shocklet structure is λ/L regardless of the flow dimension, thus an instantaneous dilatation dissipation rate (per unit mass) is

$$\epsilon_d' \propto \frac{a*^3}{L}\left(\frac{m_1^2 - 1}{m_1}\right)^3 \tag{5}$$

where $m_1 = u_1/a^*$ is the instantaneous Mach number on the low pressure side of the shock which must be larger than one. We note that the expression (5) does not contain viscosity explicitly and resembles a parametric expression for the solenoidal dissipation at low speeds (except that (5) is applicable only when m_1 is supersonic). Since the model assumes isotropic orientation of the shocklets, u_1 must be proportional to the instantaneous total turbulent velocity $u(t) = \sqrt{u_j u_j}$. In order to obtain an average value ϵ_d, (5) has to be ensemble-averaged with the aid of probability density function for m_1.

There exists experimental evidence that in mixing layers the streamwise fluctuations are highly intermittent with the kurtosis $K = \overline{u^4}/(\overline{u^2})^2$ ranging from 4 up to about 20 at the edges of the layer (Spencer and Jones 1971, Samimy et al. 1989). A convenient expression for non-gaussian p.d.f. $p(u)$ is a Gram-Charlier expansion

$$p(u, K) = \{\frac{1}{\sqrt{2\pi}} + \frac{(K-3)}{4!}\left(3 - 6\left(\frac{u}{\sigma}\right)^2 + \left(\frac{u}{\sigma}\right)^4\right)\}\exp\{-\frac{u^2}{2\sigma^2}\} \tag{6}$$

With the approximation that (6) is the p.d.f. of m_1, i.e. $p(u) \approx p(m_1)$ (with $\sigma = q/a* = M_t$), we obtain

$$\epsilon_d \propto \frac{q^3}{L}[(\frac{1}{M_t^4}\int_1^\infty \left(\frac{m_1^2 - 1}{m_1}\right)^3 p(m_1)dm_1], \quad \text{or,} \tag{7}$$

$$\epsilon_d \propto \left(\frac{q^3}{L}\right) F(M_t, K). \tag{8}$$

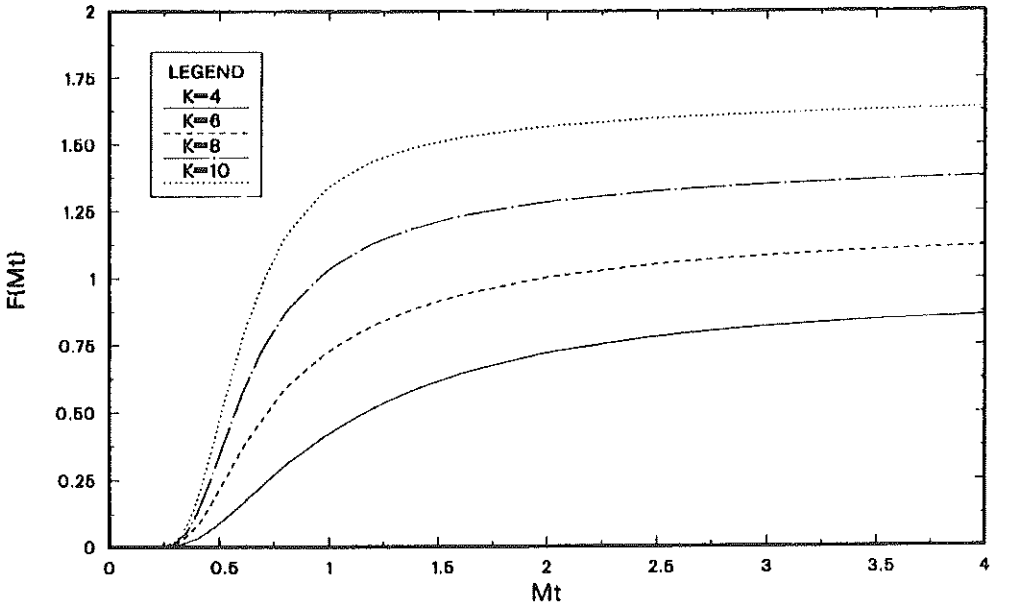

FIGURE 2. Dilatation dissipation function $F(M_t, K)$ for various values of K in the p.d.f. equation (6).

The function $F(M_t, K)$ represents the expression in square brackets above; its values obtained by numerical integration are plotted in Figure 2 for various values of the kurtosis K (in the p.d.f. equation (6). According to (8), ϵ_d is proportional to the solenoidal dissipation since $\epsilon_s \propto q^3/L$. Hence, in a second-order closure model which usually contains an equation for ϵ_s (or for L), ϵ_d is determined merely by the function $F(M_t, K)$, and the total dissipation in (1) and (2) is then

$$\epsilon_{tot} = \epsilon_s(1 + c_d F(M_t, K))$$

as suggested by dimensional analysis mentioned earlier. Apart from the model constant c_d and K (to be estimated from measurements), the total compressible turbulence dissipation is thus determined by (7) and a (standard) model equation for ϵ_s .

2.1.3. Comparison with shear layer experiments

A comparison of the dilatation dissipation model with homogenous turbulence data at sufficiently high Reynolds and Mach numbers is not possible at present. Instead, the model is compared with the experimental data in compressible free shear layers which are the least contaminated by low Reynolds number effects. For this purpose, a computer program for compressible, high Reynolds number

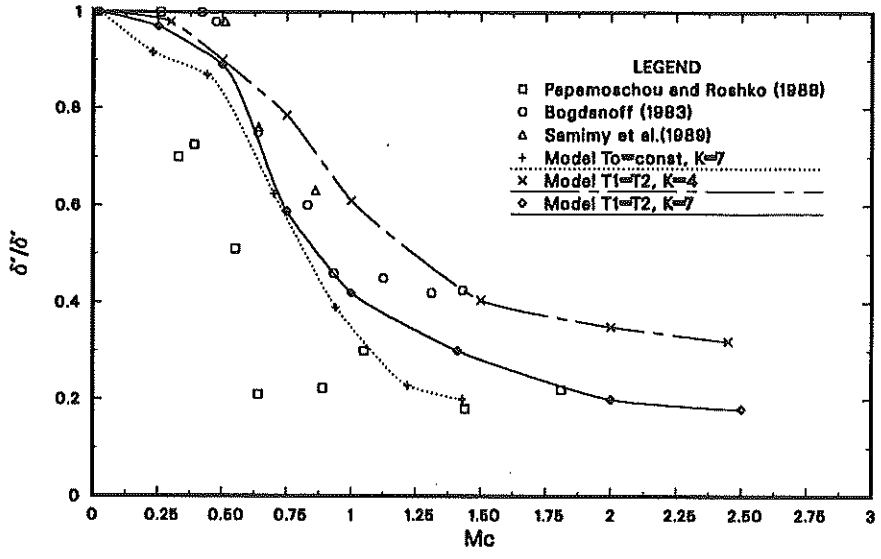

FIGURE 3. Comparison of mixing layer normalized growth rates vs. M_c.

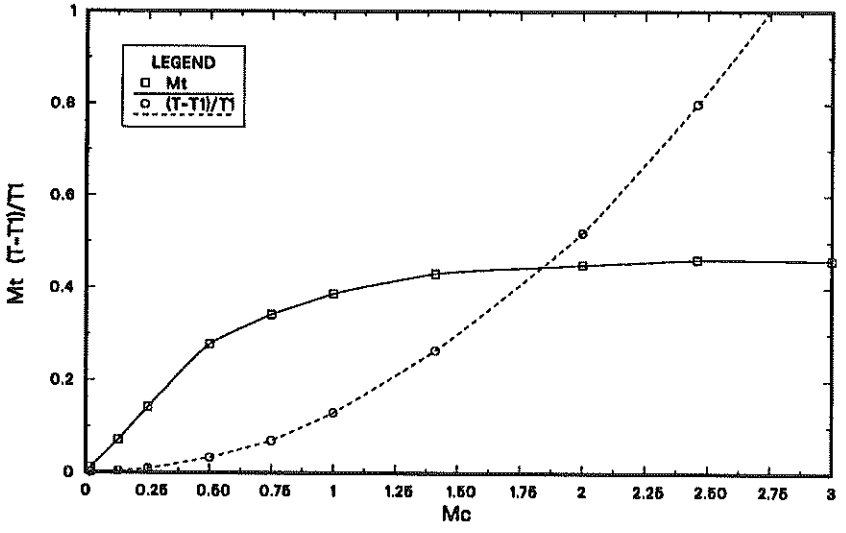

FIGURE 4. Turbulent Mach number M_t and maximum temperature excess as functions of M_c, with $T_1 = T_2$.

shear flows was formulated (Zeman, 1989) to solve transport equations for all non-zero Favre-averaged Reynolds stresses and for the vertical enthalpy flux.

The numerical scheme utilizes the von Mises transformation from (x, y) to

(x, ψ) coordinate system and all transport equations are solved by forward integration in streamwise direction x along streamlines $\psi = const.$

The crucial test of the dilation dissipation model is the prediction of the normalized growth rate δ'/δ'_o as a function of the so-called convective Mach number M_c (δ'_o is the growth rate in the incompressible limit $M_c = 0$). The concept of convective Mach number has been described in Bogdanoff (1983) and Papamoschou and Roshko (1987). With air as the (perfect) fluid, the values of δ'/δ'_o were computed for three cases: a) uniform (freestream) temperature $T_1 = T_2$ (density ratio $s = \rho_2/\rho_1$), and the kurtosis $K = 7$; b) uniform total temperature T_o, and $K = 7$; and c) uniform temperature as in case a) but with low kurtosis $K = 4$. The predicted and experimental growth rates δ'/δ'_o are compared in Figure 3. The comparison shows that the model yields realistic reduction of the shear layer growth rate as a function of the convective Mach number M_c even for small kurtosis. Figure 4 demonstrates how turbulence fluctuations are controlled by the dilatational dissipation: as M_c increases beyond one, the r.m.s. Mach number M_t appears to approach a saturation limit of about 0.5; this is observed in experiments (Samimy 1989). Figures 5, 6, and 7 display model comparisons of mean velocity, and turbulent intensities with experiments of Samimy and Elliott (1989) and Samimy et al. (1989).

Figure 5 compares the computed and experimental mean velocity profiles at two values of M_c. The profiles are shown to be universal functions of the transverse distance $(y - y_c)$ scaled by the vorticity thickness as suggested by Samimy and Elliott.

The streamwise intensity profiles are compared in Figure 6. Considering the uncertainties associated with measurements and modeling of high Mach number flows the model-experiment agreement is relatively good. Note that the measured intensities exterior to the mixing layer are due to the unavoidable background noise levels in supersonic wind tunnels.

Figure 7 compares equilibrium turbulence intensities (at the layer centerline $y = y_c$); although the model overestimates the absolute values of the intensities, the attenuation of velocity fluctuations with increasing M_c is predicted. This comparison corroborates our hypothesis that the reduction in growth rates of high speed mixing layer is a consequence of additional (dilatational) dissipation which arises due to the formation of steep density gradients, or shocklets.

2.1.4. Conclusions

We conclude with the following observations:

(1) As evident from Figure 4, the dilatation dissipation provides the controlling mechanism that suppresses excessive supersonic fluctuations and thus maintains the maximum level of the r.m.s. Mach number M_t below a certain (subsonic) level of about 0.5. This is observed in experiments. Apparently, the local intermittent shock events provide the needed dissipation to maintain, on average, turbulent velocities subsonic.

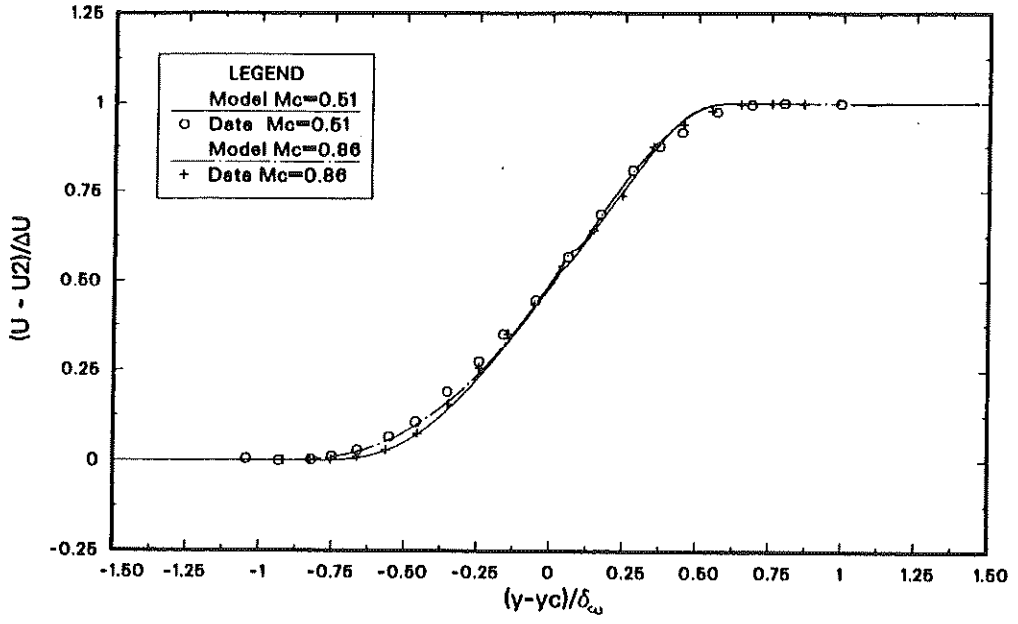

FIGURE 5. Model-experiment comparison: Mean velocity profiles at two values of M_c; abscissa is transverse distance from the layer centerline ($y = y_c$) scaled by the vorticity thickness δ_ω. Data points are from Samimy et al.(1989).

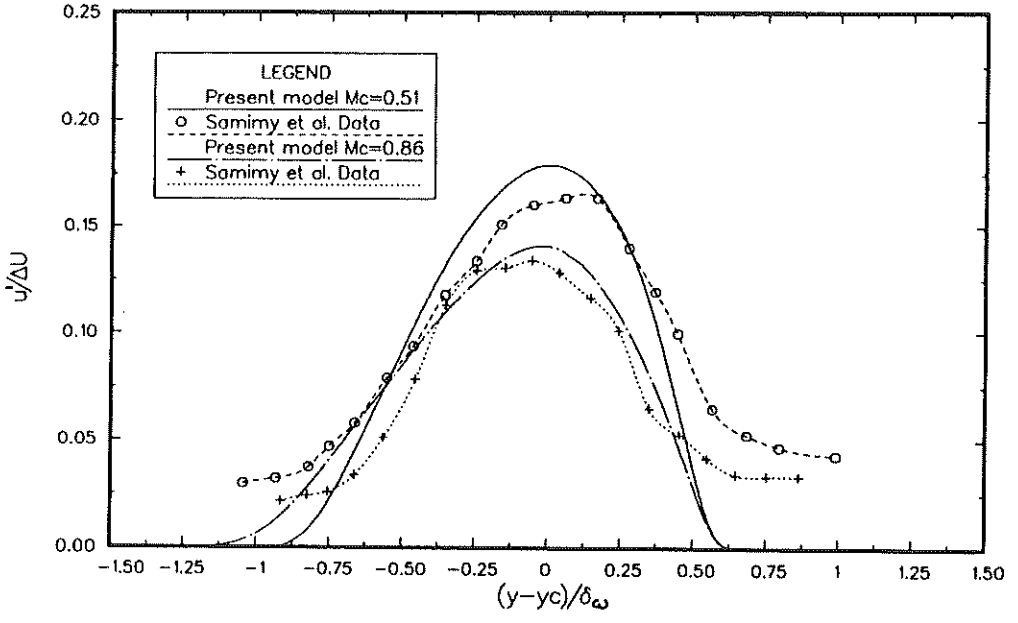

FIGURE 6. Streamwise intensity profiles, otherwise the same as Fig. 5.

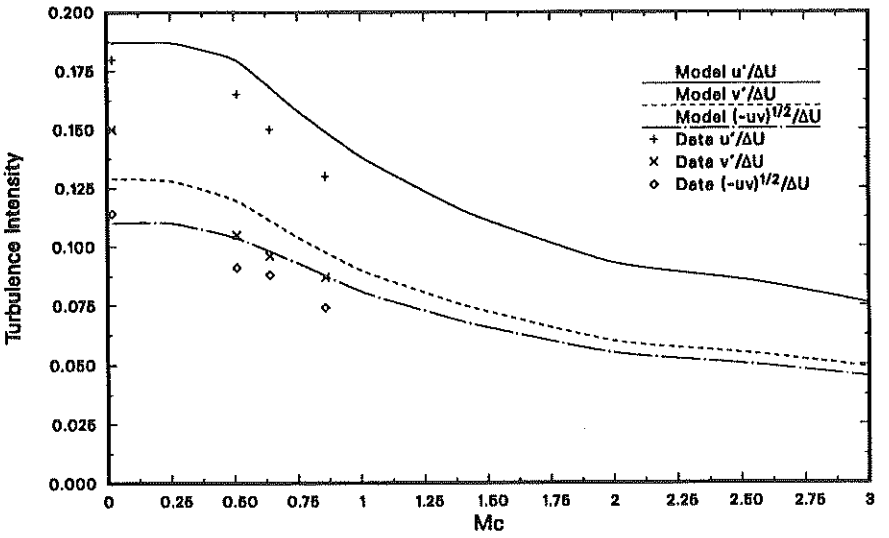

FIGURE 7. Centerline turbulence intensities vs. M_c. u', v' are r.m.s. streamwise and transverse velocities. Lines are from model predictions. Symbols are from experiments of Samimy et al. (1989).

(2) The mechanism of shock formation and dilatation dissipation bypasses the Kolmogorov energy cascade, and the process of spectral energy transfer to small scales is expected to remain unaffected by the formation of shock structures. Hence, the model equation for the solenoidal dissipation is assumed to retain its standard form independent of the dilatation dissipation.

(3) The decomposition of velocities into dilatational and solenoidal components is unique only in a strictly homogeneous turbulence field. In a bounded turbulent flow, the decomposition is not unique because of the boundary conditions. Nevertheless, the concept of the dilatation dissipation is valid, in general. The dilatation dissipation model is Galilean invariant and, therefore, applicable in any high Mach number flows such as wakes, jets, and boundary layers.

2.2 Decay of 2D compressible turbulence

In 2D turbulence the solenoidal dissipation ϵ_s is proportional to $(q^3/L)R_e^{-1}$, where the Reynolds number $R_e = qL/\nu$. Hence, according to equations (1), (2), and (8) in Section 2.1, the governing second-moment equations in 2D compressible decaying turbulence are

$$\frac{\partial q^2}{\partial t} = -\left(q^3/L\right)\{c_s R_e^{-1} + c_d F(M_t, K)\}, \tag{9}$$

$$c_p T + \frac{q^2}{2} = const. \tag{10}$$

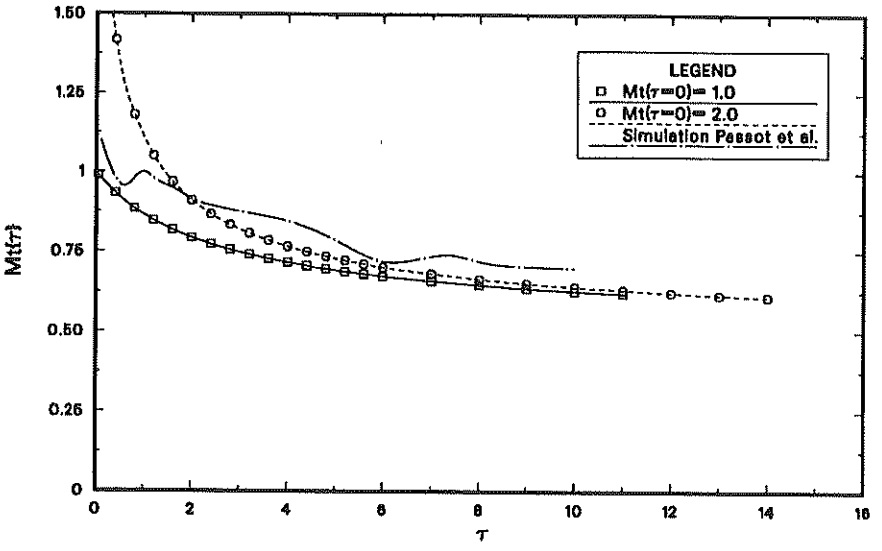

FIGURE 8. Decay of 2D homogeneous turbulence: Comparison of the decay law (11) with DNS results.

Now, (9) and (10) can be combined into a single equation for M_t^2; if, in addition, R_e is assumed to be large, the resulting equation for M_t^2 is

$$\frac{\partial M_t^2}{\partial \tau} = -2c_d M_t^2 F(M_t, K)\{1 + M_t^2 \frac{(\gamma - 1)}{2}\} \tag{11}$$

where $\tau = tq/L$ is a nondimensional time. The above equation can be considered as a *decay law* for 2D compressible turbulence. The equation can be used to verify the dilatation dissipation model when eddy shocklets are limited to 2D motion.

According to (11), for a given value of the kurtosis K, M_t decays as long as $F(M_t)$ remains sufficiently large. Since the homogeneous turbulence p.d.f.'s are gaussian, $K = 3$ and according to Figure 2 $F(M_t, K = 3)$ is negligibly small for $M_t \leq 0.4$. In Figure 8 the evolution of $M_t(\tau)$ according to (11) is tentatively compared with the DNS of 2D turbulence in molecular clouds (where $R_e >> 1$) reported by Passot et al. (1988). For comparison, we used two different initial values for M_t. It is seen that the decay law (11) yields qualitatively the same behavior as the DNS computations. In particular, the asymptotic leveling off of M_t for $\tau > 8$ is well reproduced by (11). Note that the final (asymptotic) value of M_t computed from (11) is independent of the initial conditions. This suggests that in 2D turbulence at high R_e, the dissipation is solely due to the presence of shock-like structures whose formation ceases as M_t drops below certain level. This is in agreement with the proposed theory of dilatation dissipation.

3. Current and future work

Currently, a model is being developed to simulate a hypersonic turbulent boundary layer (TBL) on a flat plate. The major concern here is to formulate a realistic model for the viscous sublayer which, in a hypersonic regime, occupies a significant portion of the total TBL thickness. Furthermore, in the hypersonic regime at freestream Mach numbers, say, $Ma_e > 15$, it is anticipated that pressure and density fluctuations, and shocklet dissipation will play a significant role in the TBL momentum and heat transfer; these issues are presently studied theoretically. Among problems to be addressed in the future are:

1) inclusion of density fluctuation equation in models of compressible and variable density turbulence.
2) Turbulence oblique shock interactions in the compression corner TBL flow.
3) parameterization of shocklet dissipation in subgrid scale models for large eddy simulations of compressible turbulence.

REFERENCES

BOGDANOFF, D.W. 1983 *AIAA J.* **21**, 926

PAPAMOSCHOU, D. & ROSHKO, A. 1988 *J. Fluid Mech* **197**, 453

PAPAMOSCHOU, D. 1986 *Ph. D. Dissertation,* CALTECH, Pasadena, CA

PASSOT, T. & POUQUET, A. 1987 *J. Fluid Mech* **181**, 441

PASSOT, T., A. POUQUET & P. WOODWARD 1988 *Astron. Astrophys* **197**, 228

SPENCER, B. W. & B.G. JONES 1971 *AIAA Paper no. 71-613,* Palo Alto, CA

SAMIMY, M. & G. S. ELLIOTT 1989 to appear in *AIAA J.*

SAMIMY, M., ERWIN, D. E. & ELLIOT, G. S. 1989 *AIAA paper no. 89-2460,* Monterey CA

ZEMAN, O. 1989 to appear in *Phys. Fluids A., Vol. 2, #2*